Relativistic distorted-wave analysis of quasielastic proton-nucleus scattering

N. P. Titus,* B. I. S. van der Ventel,† and D. D. van Niekerk‡
Department of Physics, University of Stellenbosch, Private Bag X1, Matieland 7602, South Africa

G. C. Hillhouse§
University for Information Science and Technology, Partizanska Street, Ohrid 6000, Republic of Macedonia
(Received 25 October 2010; revised manuscript received 3 February 2011; published 25 April 2011)

A relativistic distorted-wave impulse approximation formalism is presented for the calculation of quasielastic proton-nucleus scattering. It is shown that the double differential cross section may be written as a contraction between the hadronic tensor (describing the projectile and ejectile) and the polarization tensor (describing the nuclear target) and that this mathematical structure also holds for the case where distortions are included. The eikonal approximation is used to introduce distortions in the wave functions, and the nuclear response is described using a Fermi gas model. The highly oscillatory nine-dimensional integrand contained in the expression for the double differential cross section is computed using a novel technique based on combining traditional Gaussian integration methods with the powerful fitting functions in the MATLAB programming language. This work has successfully calculated the distorted-wave quasielastic differential cross section for proton-nucleus scattering within a fully relativistic framework. It is found that the distortions lead to a reduction in the double differential cross section and have a negligible effect on the computed spin observables.

DOI: 10.1103/PhysRevC.83.044616 PACS number(s): 24.10.Jv, 24.10.Eq, 24.70.+s, 25.40.−h

I. INTRODUCTION

Quasielastic scattering comprises a large percentage of the inclusive proton-nucleus spectrum, and it is therefore very important to have a quantitative description of this process. In addition, different parts of the NN interaction can be probed by studying quasielastic $(\vec{p}, \vec{p}\,')$ or $(\vec{p}, \vec{n})$ scattering. In addition to the cross section, polarization observables can be measured, which has led to a number of investigations of this reaction. The complete set of spin observables are the analyzing power A_y and the polarization transfer observables $D_{i'j}$. In particular, it was the analyzing power which proved a most useful observable in encouraging the use of a relativistic formulation (i.e., the dynamics of the reaction is based on the Dirac equation and not the traditional Schrödinger equation) of nuclear physics reactions.

The first relativistic model of quasielastic proton-nucleus scattering was formulated by Horowitz and Murdoch and was called the relativistic plane-wave impulse approximation (RPWIA) [1]. Their model correctly predicted the analyzing power for the $(\vec{p}, \vec{p}\,')$ reaction from ^{40}Ca at an incident beam energy of 500 MeV and laboratory scattering angle of 18° through the use of an effective nucleon mass, which is an intrinsically relativistic concept.

In particular, for any reaction the fundamental quantity which must be calculated is the invariant matrix element defined as

$$\mathcal{M} = \langle f|\hat{F}|i\rangle, \tag{1}$$

where $|i\rangle$ and $|f\rangle$ are the initial and final nuclear states, respectively, and $\hat{F}$ is the scattering operator that connects the initial and final states. The differential cross section is then simply given by

$$d\sigma = [\text{kinematic factor}] \times |\mathcal{M}|^2. \tag{2}$$

In general, the three quantities $|i\rangle$, $|f\rangle$, and $\hat{F}$ are extremely difficult to calculate. In the original model of Ref. [1] the following assumptions were made: (i) the reaction is a single-step process whereby the incident proton interacts with only one target nucleon, and (ii) the spin observables (being ratios of cross sections) are largely insensitive to distortions. Assumption (i) essentially reduced the nuclear scattering process to a two-body scattering process. Assumption (ii) significantly decreased the numerical burden since all nucleons could then be described by free-particle Dirac spinors. In this model the scattering operator $\hat{F}$ becomes the NN scattering matrix, which is a complex 16×16 matrix containing, in principle, 256 matrix elements. In the original RPWIA, $\hat{F}$ was parametrized by five complex amplitudes which could be obtained directly from experiment via the Wolfenstein amplitudes. Even though the analyzing power was well described by the effective nucleon mass, the polarization transfer observables preferred the free nucleon mass.

To do a thorough analysis of the original model of Ref. [1], Hillhouse *et al.* studied various aspects of the model in a series of papers [2–7], namely, (i) more refined self-consistent calculations of the projectile and ejectile effective masses, (ii) sensitivities of the complete set of spin observables to different five-term parametrizations of the NN interaction, (iii) new meson-exchange parameters for the relativistic NN amplitudes, (iv) medium modifications of the NN interaction and the effect on $(\vec{p}, \vec{p}\,')$ and $(\vec{p}, \vec{n})$ complete sets of spin observables, and (v) the replacement of the ambiguous

*nortin@sun.ac.za
†bventel@sun.ac.za
‡ddvniekerk@sun.ac.za
§gregory.hillhouse@uist.edu.mk

five-term parametrization of $\hat{F}$ by a general Lorentz-invariant representation.

The aforementioned papers were all based on the plane-wave assumption for the projectile and ejectile nucleons. References [5,8] suggest that the inclusion of nuclear distortion effects could be a way to address the discrepancies in the plane-wave relativistic impulse approximation.

In this paper, we begin with the most general form of the differential cross section and systematically derive the equivalent two-body form, which leads to a representation in which the inclusion of distortions can be done very naturally. This is done specifically for quasielastic proton-nucleus scattering. The polarized double differential cross section is written as a contraction between two tensors, namely, a projectile-ejectile tensor describing the projectile and ejectile and a target tensor describing the nuclear target. The "modular" form of the derived expression of the polarized double differential cross section allows one to systematically investigate effects such as distortions and different models for the nuclear target.

Another goal of this work is to provide the first calculation of quasielastic spin observables using relativistic distorted waves. Here one has to make a choice between using a full partial wave expansion or some other approximation which captures the main features of distortion effects while still allowing numerical results in a reasonable time. In this work, we employ the relativistic eikonal formalism for a number of reasons: (i) it has been successfully used in numerous studies of nuclear scattering reactions [9–13], (ii) it allows a measure of analytical tractability, which would be very difficult if one were to employ a full partial-wave expansion, and (iii) it offers a computational speed advantage compared to a full partial-wave expansion.

To end this section, we make the reader aware that the derived expression for the double differential cross section is, however, a multidimensional integral. This nine-dimensional integral carries an enormous computational time penalty, and we resort to computing an eight-dimensional integral which results in a function dependent on a single variable. A Fourier series is then used to fit this resultant function. Using the fitting function, we are able to perform the full integration and calculate the polarized double differential cross section in a reasonable amount of time. From the polarized double differential cross sections, we calculate polarization observables.

This paper is organized as follows. In Sec. II we present the formalism. In Sec. III we highlight briefly the procedure used to compute the polarized double differential cross section, and we end with our results in Sec. IV.

II. FORMALISM

A. Double differential cross section in terms of $\mathcal{M}$

The most general form of the differential cross section for the quasielastic scattering reaction is given by [14]

$$d\sigma = \frac{1}{|\mathbf{v}_1 - \mathbf{v}_2|}\left(\frac{M^2}{E_{\mathbf{k}}E_{\mathbf{k}'}}\right)(2\pi)^4\delta(k + K - k' - K') \times \frac{d^3k'}{(2\pi)^3}\frac{d^3K'}{(2\pi)^3}|\mathcal{M}|^2. \tag{3}$$

In Eq. (3), $\mathbf{v}_1$ and $\mathbf{v}_2$ are the velocities of the projectile and the target nucleus, $\mathcal{M}$ the transition matrix element for this particular reaction, M the free nucleon mass, and k, k', K and K' the asymptotic four-momenta of the projectile, ejectile nucleon, target, and residual nucleus, respectively. From Eq. (3),

$$(2\pi)^4\delta(k + K - k' - K') = 2\pi\delta(E_{\mathbf{k}} + E_{\mathbf{K}} - E_{\mathbf{k}'} - E_{\mathbf{K}'})(2\pi)^3\delta(\mathbf{k} + \mathbf{K} - \mathbf{k}' - \mathbf{K}'), \tag{4}$$

where we can perform the integration over $\mathbf{K}'$ in the three-dimensional δ function above and using

$$d^3k' = \mathbf{k}'^2\,dk'\,d\Omega = k'E_{\mathbf{k}'}\,dE'\,d\Omega', \tag{5}$$

where $dE' = d(E_{\mathbf{k}'})$ and $k' = |\mathbf{k}'|$. Equation (3) can now be written as

$$d\sigma = \frac{1}{(2\pi)^2|\mathbf{v}_1 - \mathbf{v}_2|}\left(\frac{M^2k'E_{\mathbf{k}'}\,dE'\,d\Omega'}{E_{\mathbf{k}}E_{\mathbf{k}'}}\right) \times \delta\left[\omega - E_{\mathbf{K}'} + E_{\mathbf{K}}\right]|\mathcal{M}|^2, \tag{6}$$

where the energy transfer

$$\omega = E_{\mathbf{k}} - E_{\mathbf{k}'} \tag{7}$$

is introduced. Rearranging factors, we obtain

$$d\sigma = \frac{M^2}{(2\pi)^2}\left(\frac{k'E_{\mathbf{k}'}\,dE'\,d\Omega'}{|\mathbf{v}_1 - \mathbf{v}_2|E_{\mathbf{k}}E_{\mathbf{k}'}}\right)|\mathcal{M}|^2\delta\left[\omega - (E_{\mathbf{K}'} - E_{\mathbf{K}})\right]. \tag{8}$$

Equation (8) is valid in any Lorentz system. We need to chose a reference frame, however; and since the distorted-wave functions are traditionally generated in the center-of-mass (c.m.) frame, we choose this as our reference frame. In the proton-nucleus c.m. frame, the three-momenta are defined as

$$\mathbf{k} + \mathbf{K} = \mathbf{k}' + \mathbf{K}', \tag{9}$$

which implies that the scattering four-momenta are then

$$\begin{aligned} k &= (E_{\mathbf{k}}, \mathbf{k}), \quad & K &= (E_{\mathbf{k}}, -\mathbf{k}), \\ k' &= (E_{\mathbf{k}'}, \mathbf{k}'), \quad & K' &= (E_{\mathbf{k}'}, -\mathbf{k}'). \end{aligned} \tag{10}$$

From the conservation of energy

$$(\mathbf{k}^2 + M^2)^{\frac{1}{2}} + \left(\mathbf{k}^2 + M_t^2\right)^{\frac{1}{2}} = (\mathbf{k}'^2 + M^2)^{\frac{1}{2}} + \left(\mathbf{k}'^2 + M_t^2\right)^{\frac{1}{2}}, \tag{11}$$

it is clear that

$$k = k'. \tag{12}$$

Equation (8) now reads

$$d\sigma = \frac{M^2}{(2\pi)^2}\left(\frac{k\,dE'\,d\Omega'}{|\mathbf{v}_1 - \mathbf{v}_2|E_{\mathbf{k}}}\right)|\mathcal{M}|^2\delta[\omega - (E_{\mathbf{K}'} - E_{\mathbf{K}})]. \tag{13}$$

We eliminate the velocity-dependent term by making the following algebraic replacement [15]:

$$|\mathbf{v}_1 - \mathbf{v}_2| \cdot [E_{\mathbf{k}}]_{\text{proj}} = \frac{k\left[(\mathbf{k}^2 + M^2)^{\frac{1}{2}} + \left(\mathbf{k}^2 + M_t^2\right)^{\frac{1}{2}}\right]}{\left(\mathbf{k}^2 + M_t^2\right)^{\frac{1}{2}}}. \tag{14}$$

Finally we replace and cancel terms in Eq. (13), which results in

$$d\sigma = \frac{M^2}{(2\pi)^2}\left(\frac{\left(\mathbf{k}^2+M_t^2\right)^{\frac{1}{2}}\, dE'\, d\Omega'}{\left[\left(\mathbf{k}^2+M^2\right)^{\frac{1}{2}}+\left(\mathbf{k}^2+M_t^2\right)^{\frac{1}{2}}\right]}\right) \times |\mathcal{M}|^2\delta\left[\omega-(E_{\mathbf{K}'}-E_{\mathbf{K}})\right]. \tag{15}$$

Grouping kinematic terms together and summing over all final nuclear states (here we replace $E_{\mathbf{K}}$ with E_0 and $E_{\mathbf{K}'}$ with E_n),

$$\frac{d\sigma}{dE'\,d\Omega'} = \left(\frac{M^2\left(\mathbf{k}^2+M_t^2\right)^{\frac{1}{2}}}{4\pi^2\left[\left(\mathbf{k}^2+M^2\right)^{\frac{1}{2}}+\left(\mathbf{k}^2+M_t^2\right)^{\frac{1}{2}}\right]}\right) \times \sum_n |\mathcal{M}|^2\delta[\omega-(E_n-E_0)]. \tag{16}$$

We now rewrite Eq. (3) in terms of the double differential cross section as

$$\frac{d\sigma}{dE'd\Omega'} = K\ \sum_n |\mathcal{M}|^2\ \delta(\omega-(E_n-E_0)), \tag{17}$$

where

$$K\ =\ \frac{M^2\left(\mathbf{k}^2+M_t^2\right)^{\frac{1}{2}}}{4\pi^2\left[(\mathbf{k}^2+M^2)^{\frac{1}{2}}+\left(\mathbf{k}^2+M_t^2\right)^{\frac{1}{2}}\right]} \tag{18}$$

is a pure kinematic factor. By using the identity

$$\mathrm{Im}\left\{\frac{1}{\omega-(E_n-E_0)+i\epsilon}\right\}\ =\ -\pi\,\delta(\omega-(E_n-E_0)),$$

and keeping in mind that $|\mathcal{M}|^2$ is purely real, Eq. (17) can be written as

$$\frac{d\sigma}{dE'\,d\Omega'} = -\frac{1}{\pi}K\ \mathrm{Im}\left\{\sum_n |\mathcal{M}|^2\ \frac{1}{\omega-(E_n-E_0)+i\epsilon}\right\}. \tag{19}$$

Equation (19) is the main result for this section. $|\mathcal{M}|^2$ is a purely real quantity, but in Eq. (19), we have related the polarized double differential cross section to the matrix element. The advantage of writing it in this form is that one can relate the nuclear response to the imaginary part of the target tensor. The target tensor or polarization tensor is a many-body entity which can then be calculated using well-known many-body techniques.

B. Transition amplitude

For the scattering process under consideration, the transition matrix element $\mathcal{M}$ is given as [10]

$$\mathcal{M} = \int d^4x\, d^4x' \prod_{i=1}^{A} d^4y_i \prod_{j=1}^{A} d^4y'_j [\bar{\psi}^{(-)}(x',\mathbf{k}',\hat{\mathbf{i}}',s') \otimes \bar{\Phi}_f(y'_1,\ldots,y'_j,\ldots,y'_A)] \times \hat{F}_{\mathrm{many}}(x,x',\{y\},\{y'\})[\psi^{(+)}(x,\mathbf{k},\hat{\mathbf{i}},s) \otimes \Phi_i(y_1,\ldots,y_i,\ldots,y_A)]. \tag{20}$$

In Eq. (20), the following notation applies:

(i) x, x', y and y' are four-vectors.
(ii) $\otimes$ denotes the Kronecker product.
(iii) $\psi^{(+)}(x,\mathbf{k},\hat{\mathbf{i}},s)$ is the relativistic distorted-wave function of the projectile with outgoing boundary conditions indicated by the superscript $(+)$ and with asymptotic three-momentum $\mathbf{k}$ in the proton-nucleus c.m. system and spin projection s along an arbitrary quantization axis $\hat{\mathbf{i}}$ in the rest frame of the projectile.
(iv) $\bar{\psi}^{(-)}(x',\mathbf{k}',\hat{\mathbf{i}}',s') = \psi^{\dagger(-)}(x',\mathbf{k}',\hat{\mathbf{i}}',s')\gamma^0$, where $\psi^{(-)}(x',\mathbf{k}',\hat{\mathbf{i}}',s')$ is the relativistic distorted-wave function of the ejectile nucleon, with incoming boundary conditions denoted by the superscript $(-)$ with asymptotic three-momentum $\mathbf{k}'$ in the nucleon-nucleus c.m. system and spin projection s' along an arbitrary quantization axis $\hat{\mathbf{i}}'$ in the rest frame of the ejectile.
(v) $\Phi_i(y_1,\ldots,y_i,\ldots,y_A)$ is the initial ground state wave function of the nucleus; a function of all A constituent target nucleons.
(vi) $\bar{\Phi}_f(y'_1,\ldots,y'_j,\ldots,y'_A)$ is the final ground state wave function of the nucleus; a function of all A constituent target nucleons.
(vii) $\hat{F}_{\mathrm{many}}(x,x',\{y\},\{y'\})$ is the operator that connects the initial and final states.

We now give our conventions for the Fourier transforms used in the analysis to follow. The Fourier transform of $f(k)$ where k is a four-vector is defined as

$$f(x) = \int \frac{d^4k}{(2\pi)^4} e^{-ik\cdot x} f(k), \tag{21}$$

and the inverse transform is

$$f(k) = \int d^4x e^{ik\cdot x} f(x). \tag{22}$$

It follows that

$$\delta(x-x') = \int \frac{d^4k}{(2\pi)^4} e^{-ik\cdot(x-x')}, \tag{23}$$

and

$$(2\pi)^4\delta(k-k') = \int d^4x e^{-ix\cdot(k-k')}. \tag{24}$$

The completeness relation is

$$1 = \int \frac{d^4p}{(2\pi)^4}|p\rangle\langle p|, \tag{25}$$

from which we obtain

$$\langle x|x'\rangle = \int \frac{d^4p}{(2\pi)^4}\langle x|p\rangle\langle p|x'\rangle = \delta(x-x'), \tag{26}$$

as well as

$$\langle x|p\rangle = e^{-ip\cdot x}, \tag{27}$$

$$\langle p|x'\rangle = e^{ip\cdot x'}. \tag{28}$$

From the experimental evidence, quasielastic scattering is a single-step reaction where the projectile is assumed to interact

with only *one bound* target nucleon in the target nucleus. The other nucleons are assumed to remain frozen during the scattering process. We approximate our $\hat{F}_{\text{many}}$ operator as

$$\hat{F}_{\text{many}}(x,x',\{y\},\{y'\}) = \sum_{i=1}^{A}\langle x' y_i'|\hat{F}|xy_i\rangle \prod_{j=1,j\neq i}^{A}\delta(y_j'-y_j), \tag{29}$$

where $\hat{F}$ is now a *two-body* operator connecting the initial and final states. Inserting this two-body operator into Eq. (20) results in

$$\begin{aligned}\mathcal{M} = \sum_{i=1}^{A}\int d^4x\ d^4x'\ d^4y_i\, d^4y_i' \left(\prod_{j=1,j\neq i}^{A} d^4y_j'\delta(y_j'-y_j)\right)\\ \times [\bar{\psi}^{(-)}(x',\mathbf{k}',\hat{\mathbf{i}}',s')\otimes\bar{\Phi}_f(y_1',\ldots,y_i',\ldots,y_A')]\\ \times\langle x' y_i'|\hat{F}|xy_i\rangle[\psi^{(+)}(x,\mathbf{k},\hat{\mathbf{i}},s)\\ \otimes\Phi_i(y_1,\ldots,y_i,\ldots,y_A)].\end{aligned} \tag{30}$$

Next we change the basis from position space to momentum space by inserting a complete set of momentum eigenstates. The bra-ket portion on the right-hand side of Eq. (29) becomes

$$\begin{aligned}\sum_{i=1}^{A}\langle x' y_i'|\hat{F}|xy_i\rangle = \sum_{i=1}^{A}\int \frac{d^4p}{(2\pi)^4}\frac{d^4p'}{(2\pi)^4}\frac{d^4p_i}{(2\pi)^4}\frac{d^4p_i'}{(2\pi)^4}\\ \times e^{ip\cdot x}e^{-ip'\cdot x'}e^{ip\cdot y_i}e^{-ip_i'\cdot y_i'}\langle p' p_i'|\hat{F}|pp_i\rangle.\end{aligned} \tag{31}$$

Substituting Eq. (31) into Eq. (30),

$$\begin{aligned}\mathcal{M} = \sum_{i=1}^{A}\int d^4x\, d^4x'\, d^4y_i\, d^4y_i' \left(\prod_{j=1,j\neq i}^{A} d^4y_j'\,\delta(y_j'-y_j)\right)\\ \times\int \frac{d^4p}{(2\pi)^4}\frac{d^4p'}{(2\pi)^4}\frac{d^4p_i}{(2\pi)^4}\frac{d^4p_i'}{(2\pi)^4}\\ \times e^{ip\cdot x}e^{-ip'\cdot x'}e^{ip\cdot y_i}e^{-ip_i'\cdot y_i'}[\bar{\psi}^{(-)}(x',\mathbf{k}',\hat{\mathbf{i}}',s')\\ \otimes\bar{\Phi}_f(y_1',\ldots,y_i',\ldots,y_A')]\\ \times\langle p' p_i'|\hat{F}|pp_i\rangle[\psi^{(+)}(x,\mathbf{k},\hat{\mathbf{i}},s)\\ \otimes\Phi_i(y_1,\ldots,y_i,\ldots,y_A)].\end{aligned} \tag{32}$$

We assume that the time dependence of the distorted incoming and outgoing wave functions are given by

$$\psi^{(+)}(x,\mathbf{k},\hat{\mathbf{i}},s) = e^{-iE_{\mathbf{k}}x_0}\psi^{(+)}(\mathbf{x},\mathbf{k},\hat{\mathbf{i}},s), \tag{33}$$

$$\bar{\psi}^{(-)}(x',\mathbf{k}',\hat{\mathbf{i}}',s') = e^{iE_{\mathbf{k}'}x_0'}\bar{\psi}^{(-)}(\mathbf{x}',\mathbf{k}',\hat{\mathbf{i}}',s'). \tag{34}$$

In a similar way, we can write down the time dependence for the initial

$$\begin{aligned}&\Phi_i(y_1,\ldots,y_i,\ldots,y_A)\\ &\quad=\left[\prod_{j=1,j\neq i}^{A} e^{-iK_{j,0}y_{j,0}}\right]e^{-iK_{i,0}y_{i,0}}\Phi_i(\mathbf{y}_1,\ldots,\mathbf{y}_i,\ldots,\mathbf{y}_A),\end{aligned} \tag{35}$$

and final nuclear target ground state wave functions

$$\begin{aligned}&\bar{\Phi}_f(y_1',\ldots,y_i',\ldots,y_A')\\ &\quad=\left[\prod_{j=1,j\neq i}^{A} e^{iK'_{j,0}y'_{j,0}}\right]e^{iK'_{i,0}y'_{i,0}}\bar{\Phi}_f(\mathbf{y}_1',\ldots,\mathbf{y}_i',\ldots,\mathbf{y}_A').\end{aligned} \tag{36}$$

Inserting the above into Eq. (32) and separating the temporal components from the spatial components results in

$$\begin{aligned}\mathcal{M} = \sum_{i=1}^{A}\Delta_i\int d^3x\, d^3x'\, d^3y_i\, d^3y_i'\frac{d^3p}{(2\pi)^3}\frac{d^3p'}{(2\pi)^3}\frac{d^3p_i}{(2\pi)^3}\frac{d^3p_i'}{(2\pi)^3}\\ \times e^{-i\mathbf{p}\cdot\mathbf{x}}e^{i\mathbf{p}'\cdot\mathbf{x}'}e^{-i\mathbf{p}_i\cdot\mathbf{y}_i}e^{i\mathbf{p}_i'\cdot\mathbf{y}_i'}[\bar{\psi}^{(-)}(\mathbf{x}',\mathbf{k}',\hat{\mathbf{i}}',s')\\ \otimes\bar{\Phi}_f(\mathbf{y}_1',\ldots,\mathbf{y}_i',\ldots,\mathbf{y}_A')]\langle\mathbf{p}'\,\mathbf{p}_i'|\hat{F}|\mathbf{p}\,\mathbf{p}_i\rangle\\ \times[\psi^{(+)}(\mathbf{x},\mathbf{k},\hat{\mathbf{i}},s)\otimes\Phi_i(\mathbf{y}_1,\ldots,\mathbf{y}_i,\ldots,\mathbf{y}_A)],\end{aligned} \tag{37}$$

where

$$\begin{aligned}\Delta_i = \int\left(\prod_{j=1,j\neq i}^{A} d^4y_j'\,\delta(y_j'-y_j)\right)\int dx_0\, dx_0'\, dy_{i,0}\, dy_{i,0}'\\ \times\frac{dp_0}{2\pi}\frac{dp_0'}{2\pi}\frac{dp_{i,0}}{2\pi}\frac{dp_{i,0}'}{2\pi}e^{-iE_{\mathbf{k}}x_0}e^{iE_{\mathbf{k}'}x_0'}e^{-iK_{i,0}y_{i,0}}e^{iK'_{i,0}y'_{i,0}}\\ \times\left[\prod_{m=1,m\neq i}^{A} e^{-iK_{m,0}y_{m,0}}\right]\left[\prod_{n=1,n\neq i}^{A} e^{iK'_{n,0}y'_{n,0}}\right]\\ \times e^{ip_o\cdot x_0}e^{-ip_o'\cdot x_0'}e^{ip_{i,o}\cdot y_{i,0}}e^{-ip'_{i,o}\cdot y'_{i,0}}.\end{aligned} \tag{38}$$

Up until now, the derivation is completely general. To progress further, we must choose a representation for the two-body operator $\hat{F}$. We choose the IA1 representation for which

$$\begin{aligned}\langle\mathbf{p}'\,\mathbf{p}_i'|\hat{F}|\mathbf{p}\,\mathbf{p}_i\rangle = (2\pi)^3\delta(\mathbf{p}+\mathbf{p}_i-\mathbf{p}'-\mathbf{p}_i')\\ \times\sum_{L=S}^{T}F_L(\mathbf{p},\mathbf{p}_i,\mathbf{p}',\mathbf{p}_i')(\lambda^L\otimes\lambda_L).\end{aligned} \tag{39}$$

In Eq. (39), the following holds true:

(i) Three-momentum conservation is explicitly enforced: $\mathbf{p}+\mathbf{p}_i=\mathbf{p}'+\mathbf{p}_i'$.

(ii) $\lambda^L\in\{I_4,\gamma^5,\gamma^\mu,\gamma^5\gamma^\mu,\sigma^{\mu\nu}\}$ where $L=S,P,V,A,T$. This is the well-known SPVAT or IA1 form of the scattering operator. Ambiguities associated with this form of $\hat{F}$ were first pointed out in Refs. [16,17]; however, this representation was successfully employed in elastic [18,19], quasielastic [1,5], and inelastic proton-nucleus scattering [10,12,20].

(iii) F_L is the complex NN amplitude.

Our model presented in this paper uses the IA1 representation due to the following reasons. Even though one should in principle use the more complete IA2 representation, this may not be the best place to start. The inclusion of distortions leads to many numerical complications, and if one were to combine this with the IA2 form it could be very difficult to disentangle different effects. From a pedagogical point of view, it is therefore best to first use the IA1 representation. A numerical implementation of the IA2 representation is a very

complicated undertaking, as shown in the work of Tjon and Wallace and Van der Ventel *et al.* In addition, one can argue that the IA1 calculation should always serve as a baseline for the full IA2 calculation, since the latter contains the SPVAT form as a special case.

Inserting Eq. (39) into Eq. (37) and performing the integration over the undetected recoil nucleus momentum $\mathbf{p}_i'$ and substituting the result into Eq. (37) results in

$$\begin{aligned}\mathcal{M} = \sum_{i=1}^{A}\Delta_i \sum_{L=S}^{T}\int d^3x\, d^3x'\, d^3y_i\, d^3y_i' \frac{d^3p}{(2\pi)^3}\frac{d^3p'}{(2\pi)^3}\frac{d^3p_i}{(2\pi)^3} \\ \times e^{-i\mathbf{p}(\mathbf{y}_i-\mathbf{x})}e^{i\mathbf{p}'(\mathbf{x}'-\mathbf{y}_i')}e^{-i\mathbf{p}_i(\mathbf{y}_i'-\mathbf{y}_i)}[\bar{\psi}^{(-)}(\mathbf{x}',\mathbf{k}',\hat{\mathbf{i}}',s') \\ \otimes \bar{\Phi}_f(\mathbf{y}_1',\ldots,\mathbf{y}_i',\ldots,\mathbf{y}_A')]F_L(\mathbf{p},\mathbf{p}_i,\mathbf{p}')(\lambda^L\otimes\lambda_L) \\ \times[\psi^{(+)}(\mathbf{x},\mathbf{k},\hat{\mathbf{i}},s)\otimes\Phi_i(\mathbf{y}_1,\ldots,\mathbf{y}_i,\ldots,\mathbf{y}_A)]. \quad (40)\end{aligned}$$

The relativistic free NN scattering amplitudes are normally extracted from free NN scattering experiments via suitable phase-shift analysis, such as the well-known Arndt phases [21]. The explicit dependence of $\hat{F}$ on the "local" momenta $\mathbf{p}$, $\mathbf{p}_i$, and $\mathbf{p}'$ in Eq. (40) is thereby replaced by the corresponding asymptotic values $\mathbf{k}$, $\mathbf{K}_i$, and $\mathbf{k}'$. Hence we make the replacement

$$F_L(\mathbf{p},\mathbf{p}_i,\mathbf{p}') \longrightarrow F_L(\mathbf{k},\mathbf{K}_i,\mathbf{k}'). \quad (41)$$

The only dependence on the momenta $\mathbf{p}$, $\mathbf{p}_i$, and $\mathbf{p}'$ are now buried in the exponentials, and we can systematically perform the integrals over these variables, i.e.,

$$\int d^3p\, e^{-i\mathbf{p}\cdot(\mathbf{y}_i-\mathbf{x})} = (2\pi)^3\delta(\mathbf{y}_i-\mathbf{x}). \quad (42)$$

The result is a product of δ functions of the form

$$\delta(\mathbf{x}'-\mathbf{y}_i')\delta(\mathbf{y}_i-\mathbf{x})\delta(\mathbf{y}_i'-\mathbf{y}_i). \quad (43)$$

Equation (40) becomes

$$\begin{aligned}\mathcal{M} = \sum_{i=1}^{A}\Delta_i\sum_{L=S}^{T}\int d^3x\, d^3x'\, d^3y_i\, d^3y_i' \\ \times\delta(\mathbf{x}'-\mathbf{y}_i')\delta(\mathbf{y}_i-\mathbf{x})\delta(\mathbf{y}_i'-\mathbf{y}_i) \\ \times[\bar{\psi}^{(-)}(\mathbf{x}',\mathbf{k}',\hat{\mathbf{i}}',s')\otimes\bar{\Phi}_f(\mathbf{y}_1',\ldots,\mathbf{y}_i',\ldots,\mathbf{y}_A')] \\ \times F_L(\mathbf{k},\mathbf{K}_i,\mathbf{k}')(\lambda^L\otimes\lambda_L) \\ \times[\psi^{(+)}(\mathbf{x},\mathbf{k},\hat{\mathbf{i}},s)\otimes\Phi_i(\mathbf{y}_1,\ldots,\mathbf{y}_i,\ldots,\mathbf{y}_A)]. \quad (44)\end{aligned}$$

By performing the integration over $\mathbf{y}_i'$, $\mathbf{y}_i$, and $\mathbf{x}_i'$ in the three-dimensional δ functions systematically, Eq. (44) becomes

$$\begin{aligned}\mathcal{M} = \sum_{i=1}^{A}\Delta_i\sum_{L=S}^{T}\int d^3x\, F_L(\mathbf{k},\mathbf{K}_i,\mathbf{k}') \\ \times[\bar{\psi}^{(-)}(\mathbf{x},\mathbf{k}',\hat{\mathbf{i}}',s')\otimes\bar{\Phi}_f(\mathbf{y}_1',\ldots,\mathbf{x},\ldots,\mathbf{y}_A')] \\ \times(\lambda^L\otimes\lambda_L)[\psi^{(+)}(\mathbf{x},\mathbf{k},\hat{\mathbf{i}},s)\otimes\Phi_i(\mathbf{y}_1,\ldots,\mathbf{x},\ldots,\mathbf{y}_A)]. \quad (45)\end{aligned}$$

Using the identity

$$(A\otimes B)(C\otimes D) = AC\otimes BD \quad (46)$$

repeatedly Eq. (45) becomes

$$\begin{aligned}\mathcal{M} = \sum_{i=1}^{A}\Delta_i\sum_{L=S}^{T}F_L(\mathbf{k},\mathbf{K}_i,\mathbf{k}')\int d^3\mathbf{x} \\ \times[\bar{\psi}^{(-)}(\mathbf{x},\mathbf{k}',\hat{\mathbf{i}}',s')\lambda^L\psi^{(+)}(\mathbf{x},\mathbf{k},\hat{\mathbf{i}},s)] \\ \times[\bar{\Phi}_f(\mathbf{y}_1',\ldots,\mathbf{x},\ldots,\mathbf{y}_A')\lambda_L\Phi_i(\mathbf{y}_1,\ldots,\mathbf{x},\ldots,\mathbf{y}_A)]. \quad (47)\end{aligned}$$

The target space contains initial and final wave functions and is still extremely complicated. We now make an additional approximation: we assume that the operator λ_L has a simple one-body form. We can then define the initial and final nuclear states in terms of Slater determinants as

$$\Phi_i = \frac{1}{\sqrt{A!}}\det\left[\phi_n^{(i)}(\mathbf{y}_k)\right]_{n=1,\ldots,A,\ k=1,\ldots,A}, \quad (48)$$

$$\Phi_f = \frac{1}{\sqrt{A!}}\det\left[\phi_m^{(f)}(\mathbf{y}_k)\right]_{m=1,\ldots,A,\ k=1,\ldots,A}. \quad (49)$$

The action of the operator λ_L now acting on the ith particle only can then be written as

$$\begin{aligned}\int\prod_{j=1,j\neq i}^{A}d^3y_j\,\bar{\Phi}_f\lambda_L^{(i)}\Phi_i \\ = \frac{1}{A!}\sum_{m=1}^{A}\sum_{n=1}^{A}(-1)^{2+m+n}\int\prod_{j=1,j\neq i}^{A}d^3y_j\,\overline{\det\left[\phi_{g\neq m}^{(f)}(\mathbf{y}_{k\neq i})\right]} \\ \times\det\left[\phi_{h\neq n}^{(i)}(\mathbf{y}_{\ell\neq i})\right]\bar{\phi}_m^{(f)}(\mathbf{y}_i)\lambda_L^{(i)}\phi_n^{(i)}(\mathbf{y}_i). \quad (50)\end{aligned}$$

The initial and final nuclear states now differ only by a single one-particle state, for example, state number 1; this then becomes

$$\begin{aligned}\int\prod_{j=1,j\neq i}^{A}d^3y_j\,\bar{\Phi}_f\lambda_L^{(i)}\Phi_i &= \frac{(A-1)!}{A!}\sum_{m=1}^{A}\sum_{n=1}^{A}\delta_{m1}\delta_{n1}\bar{\phi}_m^{(f)}(\mathbf{y}_i) \\ &\quad\times\lambda_L^{(i)}\phi_n^{(i)}(\mathbf{y}_i) \\ &= \frac{1}{A}\bar{\phi}_1^{(f)}(\mathbf{y}_i)\lambda_L^{(i)}\phi_1^{(i)}(\mathbf{y}_i) \\ &= \frac{1}{A}\langle\Phi_f|\hat{\bar{\phi}}(\mathbf{x})\lambda_L\hat{\phi}(\mathbf{x})|\Phi_i\rangle, \quad (51)\end{aligned}$$

where $\hat{\phi}$ is the Heisenberg field operator and $\mathbf{y}_i\to\mathbf{x}$ from the preceding integrations. Finally substituting Eq. (51) into Eq. (47) gives

$$\begin{aligned}\mathcal{M} = \sum_{i=1}^{A}\frac{\Delta_i}{A}\sum_{L=S}^{T}\int d^3\mathbf{x}F_L(\mathbf{k},\mathbf{K}_i,\mathbf{k}') \\ \times[\bar{\psi}^{(-)}(\mathbf{x},\mathbf{k}',\hat{\mathbf{i}}',s')\lambda^L\psi^{(+)}(\mathbf{x},\mathbf{k},\hat{\mathbf{i}},s)] \\ \times\langle\Phi_f|\hat{\bar{\phi}}(\mathbf{x})\lambda_L\hat{\phi}(\mathbf{x})|\Phi_i\rangle, \quad (52)\end{aligned}$$

with

$$\Delta_i = 1 \Rightarrow \sum_{i=1}^{A}\Delta_i = A. \quad (53)$$

Taking the complex conjugate for $\mathcal{M}$ results in

$$\mathcal{M}^* = \sum_{L'=S}^{T} \int d^3\mathbf{y} F^*_{L'}(\mathbf{k}, \mathbf{K}_i, \mathbf{k}')[\bar{\psi}^{(+)}(\mathbf{y}, \mathbf{k}', \hat{\mathbf{i}}', s') \times \overline{\lambda^{L'}} \psi^{(-)}(\mathbf{y}, \mathbf{k}, \hat{\mathbf{i}}, s)]\langle \Phi_i | \hat{\bar{\phi}}(\mathbf{y}) \overline{\lambda_{L'}} \hat{\phi}(\mathbf{y}) | \Phi_f \rangle. \quad (54)$$

C. Hadronic tensor

Substituting Eqs. (52) and (54) into Eq. (19) results in

$$\frac{d\sigma}{dE'\, d\Omega'} = -\frac{1}{\pi} K \mathrm{Im}\left[\sum_{L,L'=S}^{T} F_L(\mathbf{k}, \mathbf{k}', \mathbf{K}) F^*_{L'}(\mathbf{k}, \mathbf{k}', \mathbf{K}) \times \int d^3x\, d^3y\, \mathcal{H}^{LL'}(\mathbf{x}, \mathbf{y}) \Pi_{LL'}(\mathbf{x}, \mathbf{y}, \omega) \right]. \quad (55)$$

In Eq. (55) the projectile-ejectile tensor $\mathcal{H}^{LL'}(\mathbf{x}, \mathbf{y})$ is defined as

$$\mathcal{H}^{LL'}(\mathbf{x}, \mathbf{y}) = [\bar{\psi}^{(-)}(\mathbf{x}, \mathbf{k}', \hat{\mathbf{i}}', s') \lambda^L \psi^{(+)}(\mathbf{x}, \mathbf{k}, \hat{\mathbf{i}}, s)] \times [\bar{\psi}^{(+)}(\mathbf{y}, \mathbf{k}, \hat{\mathbf{i}}, s) \overline{\lambda^{L'}} \psi^{(-)}(\mathbf{y}, \mathbf{k}', \hat{\mathbf{i}}', s')],$$

and the polarization tensor $\Pi_{LL'}(\mathbf{x}, \mathbf{y}, \omega)$ is defined as

$$\Pi_{LL'}(\mathbf{x}, \mathbf{y}, \omega) = \sum_n \frac{\langle n | \hat{\bar{\phi}}(\mathbf{x}) \lambda_L \hat{\phi}(\mathbf{x}) | 0 \rangle \langle 0 | \hat{\bar{\phi}}(\mathbf{y}) \overline{\lambda^{L'}} \hat{\phi}(\mathbf{y}) | n \rangle}{\omega - (E_n - E_0) + i\epsilon} + \frac{\langle n | \hat{\bar{\phi}}(\mathbf{y}) \overline{\lambda^{L'}} \hat{\phi}(\mathbf{y}) | 0 \rangle \langle 0 | \hat{\bar{\phi}}(\mathbf{x}) \lambda_L \hat{\phi}(\mathbf{x}) | n \rangle}{\omega + (E_n - E_0) - i\epsilon}. \quad (56)$$

In the nuclear matter approximation, Eq. (56) can be written as

$$\Pi_{LL'}(\mathbf{x}, \mathbf{y}, \omega) = \int \frac{d^3q}{(2\pi)^3} e^{-i\mathbf{q}\cdot(\mathbf{x}-\mathbf{y})} \Pi_{LL'}(\mathbf{q}, \omega). \quad (57)$$

Substituting Eq. (57) into Eq. (55) gives

$$\frac{d\sigma}{dE'\, d\Omega'} = -\frac{1}{\pi} K \mathrm{Im}\left[\sum_{L,L'=S}^{T} F_L(\mathbf{k}, \mathbf{k}', \mathbf{K}) F^*_{L'}(\mathbf{k}, \mathbf{k}', \mathbf{K}) \times \int \frac{d^3q}{(2\pi)^3} \mathcal{H}^{LL'}(\mathbf{q}) \Pi_{LL'}(\mathbf{q}, \omega) \right], \quad (58)$$

where the hadronic tensor $\mathcal{H}^{LL'}$ is given by

$$\mathcal{H}^{LL'}(\mathbf{q}) = \int d^3x\, d^3y\, e^{-i\mathbf{q}\cdot(\mathbf{x}-\mathbf{y})} \mathcal{H}^{LL'}(\mathbf{x}, \mathbf{y}) = \int d^3x\, e^{-i\mathbf{q}\cdot\mathbf{x}} [\bar{\psi}^{(-)}(\mathbf{x}, \mathbf{k}', \hat{\mathbf{i}}', s') \lambda^L \psi^{(+)}(\mathbf{x}, \mathbf{k}, \hat{\mathbf{i}}, s)] \times \int d^3y\, e^{i\mathbf{q}\cdot\mathbf{y}} [\bar{\psi}^{(+)}(\mathbf{y}, \mathbf{k}, \hat{\mathbf{i}}, s) \overline{\lambda^{L'}} \psi^{(-)}(\mathbf{y}, \mathbf{k}', \hat{\mathbf{i}}', s')] \quad (59)$$

$$= \mathcal{H}^L(\mathbf{q}) [\mathcal{H}^{L'}(\mathbf{q})]^*. \quad (60)$$

Equation (58) is our main result for this section. It is the double differential cross section written as a contraction of the hadronic tensor $\mathcal{H}^{LL'}$ and the polarization tensor $\Pi_{LL'}$. The hadronic tensor contains all the information pertaining to the projectile and the ejectile nucleons. The nuclear distortions are built into this quantity and will be discussed further in Secs. II C2 and II C3. What is important to note in Eq. (59) is that distortions to any level of sophistication can be incorporated in the projectile and ejectile wave functions. The consequence of this formulation in Eq. (58) of the differential cross section is that the "contraction of tensors" structure often seen in elementary particle physics also holds for the case where distortions are included. This is an important result of this work.

To summarize then, starting with the most basic form of the matrix element, the complex scattering problem is reduced to a two-body scattering problem using the SPVAT representation of the NN scattering operator $\hat{F}$ that was successfully used in proton-nucleus scattering reactions [1,5,10,12,20]. The scattering operator, formulated in momentum space, is normally evaluated at the asymptotic momenta. The amplitudes are then completely determined by free scattering data [21]. Replacing the amplitudes with their respective asymptotic momenta values allows the integrations over the local momenta to be performed. The remaining integrations over the spatial coordinates are performed, and the invariant matrix element is written in a form containing a projectile-ejectile part and a target-space part. Taking the product of the matrix element and its complex conjugate and applying the nuclear matter approximation to the target tensor resulted in the form of Eq. (58). Writing the cross section as a contraction of two tensors is analogous to what is normally done in elementary particle physics and usually all the complexity is encoded in the hadronic tensor. The compact expression for the double differential cross section given in Eq. (58), however, hides the extreme difficulty in its numerical implementation for a number of reasons:

(i) In general the hadronic tensor should be calculated using distorted waves for the projectile and ejectile. The numerical complexity associated with using distorted waves as opposed to plane waves will be further expanded upon in Sec. II C1. The standard choice here that must be made is between a full partial-wave expansion or an eikonal approximation.

(ii) The response of the nucleus to an external probe is described by the polarization tensor. This is an extremely complicated quantity but it can be evaluated systematically using various approximations.

(iii) The calculation of the multidimensional integrals d^3x, d^3y, and d^3q significantly increases the numerical burden.

(iv) The large number of Lorentz indices which must be contracted: 25 in total since $L, L' \in \{S, P, V, A, T\}$. This is in contrast to, for example, electromagnetic two-body electron-proton scattering, where one has to contract at most two Lorentz indices. To provide a systematic way of evaluating this contraction we classify the tensors according to the number of Lorentz indices they have. This is called the rank of the tensor, and the combinations which may be made up from the set $\{S, P, V, A, T\}$ by taking pairs are classified according to the rank in Table I.

The factors mentioned above have been significant in retarding progress in the analysis of quasielastic

TABLE I. Grouping of ranks of target polarizations based on the Lorentz indices needed to specify a particular polarization.

Rank	Polarization tensors			
0	Π_{SS}	Π_{SP}	Π_{PS}	Π_{PP}
1	Π_{SV}	Π_{SA}	Π_{PV}	Π_{PA}
	Π_{VS}	Π_{VP}	Π_{AS}	Π_{AP}
2	Π_{ST}	Π_{PT}	Π_{VV}	Π_{VA}
	Π_{AV}	Π_{AA}	Π_{TS}	Π_{TP}
3	Π_{VT}	Π_{AT}	Π_{TV}	Π_{TA}
4	Π_{TT}			

proton-nucleus scattering using distorted waves. In the next section we study the hadronic tensor in detail.

1. Hadronic tensor: Plane-wave case

To compute one factor of Eq. (60) is computationally very demanding in a distorted-wave formulation and therefore the plane-wave case is presented first. The position space representation of the incoming Dirac plane wave is given by

$$\psi^{(+)}(\mathbf{x},\mathbf{k},\hat{\mathbf{i}},s) = U(\mathbf{k},\hat{\mathbf{i}},s)e^{i\mathbf{k}\cdot\mathbf{x}}, \tag{61}$$

and the outgoing Dirac plane-wave spinor by

$$\psi^{(-)}(\mathbf{x},\mathbf{k}',\hat{\mathbf{i}}',s') = U(\mathbf{k}',\hat{\mathbf{i}}',s')e^{i\mathbf{k}'\cdot\mathbf{x}}, \tag{62}$$

in which the Dirac spinor is

$$U(\mathbf{k},\hat{\mathbf{i}},s) = \sqrt{\frac{E_{\mathbf{k}}+M}{2M}}\begin{bmatrix}\phi(\hat{\mathbf{i}},s)\\ \frac{\vec{\sigma}\cdot\mathbf{k}}{E_{\mathbf{k}}+M}\phi(\hat{\mathbf{i}},s)\end{bmatrix}, \tag{63}$$

with $E_{\mathbf{k}}^2 = \mathbf{k}^2 + M^2$. The Pauli spinor $\phi(\hat{\mathbf{i}},s)$ is defined as

$$\phi(\hat{\mathbf{i}},s) = \sum_{s_z}\mathcal{D}^{(1/2)}_{s_z s}(\hat{\mathbf{i}})\chi_s, \tag{64}$$

in which $\mathcal{D}^{(1/2)}_{s_z s}$ is the Wigner-D function and the polarized two-component spinor χ_s is a linear combination of $\chi_{s_z=\frac{1}{2}}$ and $\chi_{s_z=-\frac{1}{2}}$ defined as

$$\chi_s = \chi_{s_z=\frac{1}{2}} + \chi_{s_z=-\frac{1}{2}}. \tag{65}$$

The orientation of the spin polarization is obtained by performing a Wigner-D transformation on χ_s. We define the longitudinal, sideways, and normal polarization directions as $\hat{\mathbf{l}}$, $\hat{\mathbf{s}}$, and $\hat{\mathbf{n}}$, respectively. The Wigner-D function is a 2×2 matrix given in Ref. [22] as

$$\mathcal{D}^{(1/2)}_{s_z s}(\hat{\mathbf{i}}) = \begin{bmatrix} e^{-i(\alpha+\gamma)/2}\cos\frac{\beta}{2} & -e^{-i(\alpha-\gamma)/2}\sin\frac{\beta}{2}\\ e^{i(\alpha-\gamma)/2}\sin\frac{\beta}{2} & e^{i(\alpha+\gamma)/2}\cos\frac{\beta}{2}\end{bmatrix}, \tag{66}$$

in which the quantization axis $\hat{\mathbf{i}}$ represents the spin polarizations $\hat{\mathbf{l}}$, $\hat{\mathbf{s}}$, and $\hat{\mathbf{n}}$. These polarizations are related to the Euler angles used in Eq. (66) as follows for

$$\hat{\mathbf{l}}: \alpha = 0\beta = \theta_{\text{c.m.}}\gamma = 0, \tag{67}$$

$$\hat{\mathbf{s}}: \alpha = 0\beta = \pi/2 + \theta_{\text{c.m.}}\gamma = 0, \tag{68}$$

$$\hat{\mathbf{n}}: \alpha = \pi/2\beta = \pi/2\gamma = 0. \tag{69}$$

Substituting Eqs. (61) and (62) into $\mathcal{H}^L(\mathbf{q})$ and performing the integration over the d^3x and d^3y integrals results in

$$\mathcal{H}^{LL'}(\mathbf{q}) = [(2\pi)^3\delta(\mathbf{k}-\mathbf{k}'-\mathbf{q})]^2[\bar{U}(\mathbf{k}',\hat{\mathbf{i}}',s')\lambda^L U(\mathbf{k},\hat{\mathbf{i}},s)] \times[\bar{U}(\mathbf{k},\hat{\mathbf{i}},s)\overline{\lambda^{L'}}U(\mathbf{k}',\hat{\mathbf{i}}',s')]. \tag{70}$$

As an example, we give the result using the SS interaction where $L = S \to \lambda^{[L=S]} = I_4$ and trace techniques are used to evaluate Eq. (70)

$$\mathcal{H}^{SS}(\mathbf{q}) = [(2\pi)^3\delta(\mathbf{k}-\mathbf{k}'-\mathbf{q})]^2\frac{1}{16M^2}[4k\cdot k' + 4k\cdot s'k'\cdot s - 4s\cdot s'(k\cdot k'+M^2) + 4M^2]. \tag{71}$$

Substituting Eqs. (71) and (76) into Eq. (58) and performing the integration over $\mathbf{q}$ generates a leading $\delta(0)$ factor. The $\delta(0)$ factor evaluates to infinity and should strictly be computed numerically; however, one can apply a common trick, namely,

$$\delta(0) = \frac{V}{(2\pi)^3} = \frac{1}{(2\pi)^3}\left(\frac{A}{\rho_B}\right), \tag{72}$$

where ρ_B is the baryon density, and

$$\rho_B = \frac{\gamma}{6\pi^2}k_F^3, \tag{73}$$

where the degeneracy factor $\gamma = 4$ for nuclear matter. This leads to

$$\delta(0) = \frac{3\pi^2 A}{2k_F^3}, \tag{74}$$

where k_F^3 is the Fermi momentum. We then arrive at

$$\left(\frac{d\sigma}{dE'\,d\Omega'}\right)_{PW} = -\frac{1}{\pi}K(F_S(\mathbf{k},\mathbf{k}',\mathbf{K})F_S^*(\mathbf{k},\mathbf{k}',\mathbf{K}))\left(\frac{3\pi^2A}{2k_F^3}\right) \times\frac{1}{16M^2}[4k\cdot k' + 4k\cdot s'k'\cdot s - 4s\cdot s'(k\cdot k'+M^2) + 4M^2][\text{Im}\{\Pi_{SS}(\mathbf{k}-\mathbf{k}',\omega)\}], \tag{75}$$

Eq. (75) is then an analytical solution to compute the polarized double differential cross section in the plane-wave limit for the SS interaction only. The same procedure is followed to derive a similar expression to Eq. (75) using the PP interaction. The polarization tensor is based on the relativistic Fermi-gas model and treats the nuclear ground state as a system of noninteracting fermions at finite density. Note that the polarization tensors for $\text{Im}\{\Pi_{SP}\} = \text{Im}\{\Pi_{PS}\} = 0$ and for [23,24]

$$\text{Im}\{\Pi_{SS}\} = -\frac{1}{8\pi|\mathbf{q}|}(4M^{*2} - q^2)(E_F^* - E^*), \tag{76}$$

$$\text{Im}\{\Pi_{PP}\} = \frac{q^2}{8\pi|\mathbf{q}|}(E_F^* - E^*), \tag{77}$$

where M^* is the reduced mass, the four-vector $q^2 = \omega^2 - \mathbf{q}^2$, and

$$E^* = \min(E_F^*, E_{\max}), \tag{78}$$

in which

$$E_{\max} = \max\left\{E_F^* - \omega, \frac{1}{2}\left[|\mathbf{q}|\left(1 - \frac{4M^{*2}}{q^2}\right)^{\frac{1}{2}} - \omega\right]\right\}. \tag{79}$$

The quantity E_F^* is the energy at the Fermi momentum given by

$$E_F^* = \sqrt{\mathbf{k_F^2} + \mathbf{M^{*2}}}. \tag{80}$$

The polarization observables are defined as linear combinations of polarized double differential cross sections. For simplicity we let

$$d\sigma_{s_z s_z'} = \frac{d\sigma}{d\Omega' dE'}(s_i, s_f), \tag{81}$$

where $s_i = (j, s_z)$ and $s_f = (i', s_z')$ refer to the initial and final spin polarizations, respectively, and $j \in \{\hat{\mathbf{l}}; \hat{\mathbf{s}}; \hat{\mathbf{n}}\}$ and $i' \in \{\hat{\mathbf{l}}'; \hat{\mathbf{s}}'; \hat{\mathbf{n}}'\}$. We introduce the short-hand notation u to designate the spin projection direction $s_z = \frac{1}{2}$ or "spin-up" and d to designate the spin projection direction $s_z = -\frac{1}{2}$ or "spin-down." Polarization observables are then calculated as

$$D_{i'j} = \frac{d\sigma_{uu} - d\sigma_{du} - d\sigma_{ud} + d\sigma_{dd}}{d\sigma_{uu} + d\sigma_{du} + d\sigma_{ud} + d\sigma_{dd}}. \tag{82}$$

The unpolarized double differential cross section is given by the denominator in Eq. (82). The analyzing power A_y is the ratio of initially polarized nucleons left unpolarized after interacting with the target nucleus and is calculated using

$$A_y = \frac{(d\sigma_{uu} + d\sigma_{du}) - (d\sigma_{ud} + d\sigma_{dd})}{d\sigma_{uu} + d\sigma_{du} + d\sigma_{ud} + d\sigma_{dd}}. \tag{83}$$

2. Hadronic tensor: Distorted-partial-wave case

Introducing distorted waves for the projectile and ejectile in quasielastic proton-nucleus scattering represents a significant improvement over previous work [2–7,25] which utilized the plane-wave impulse approximation. A choice must be made between a full partial-wave expansion or some approximation which retains the essentials of distortion effects. To illustrate the numerical challenge one faces in calculating $\mathcal{H}^{LL'}$ using full distorted partial waves consider the partial-wave expansion of the projectile wave function [10,26–28]

$$\psi^{(+)}(\mathbf{x}, \mathbf{k}, \hat{\mathbf{i}}, s) = \frac{4\pi}{kx}\left(\frac{E_{\mathbf{k}} + M}{2M}\right)^{\frac{1}{2}} \sum_{ljm_l s_z} i^l e^{i\delta_{lj}} \left\langle l\tfrac{1}{2} m s_z | j, m + s_z \right\rangle \times \mathcal{D}^{(\frac{1}{2})}_{s_z s}(\hat{\mathbf{i}})\, Y^*_{lm}(\hat{\mathbf{x}}) \begin{bmatrix} g_{lj}(kx)\mathcal{Y}_{lj,m+s_z}(\hat{\mathbf{x}}) \\ i f_{2j-l,j}(kx)\mathcal{Y}_{2j-l,j,m+s_z}(\hat{\mathbf{x}}) \end{bmatrix}, \tag{84}$$

with a similar expression for the ejectile wave function. The above equation has the following notation:

(i) $x = |\mathbf{x}|$ and $k = |\mathbf{k}|$.
(ii) $\langle l\frac{1}{2} m_l m_s | j m_j \rangle$ is a Clebsch-Gordon coefficient.
(iii) $Y_{lm}(\hat{\mathbf{x}})$ is a spherical harmonic function.
(iv) $g_{lj}(z)$ and $f_{lj}(z)$ are radial wave function solutions of Schrodinger-like radial differential equations that contain the central, spin-orbit, and Darwin potentials [26,27].
(v) $\mathcal{Y}_{lj\mu}(\hat{\mathbf{x}})$ is a spin-spherical harmonic function given by

$$\mathcal{Y}_{lj\mu}(\hat{\mathbf{x}}) = \sum_{t_z'} \left\langle l\frac{1}{2}, \mu - t_z', t_z' | j\mu \right\rangle Y_{l,\mu - t_z'}(\hat{\mathbf{x}})\chi_{t_z'}. \tag{85}$$

(vi) The relativistic Coulomb phase shift δ_{lj} is an implicit function of the projectile and target masses, the projectile and target atomic numbers, and the momentum $\mathbf{k}$.

From Eq. (84) one can see that the incident projectile has a sum over l up to some $l_{\max}$ where typically the amount of partial waves needed to give a relatively accurate description of the distortion effects is a function of the physical size of the target nucleus, the range of the interaction, and the energies of the colliding particles. For instance, one or two partial waves will suffice in some scattering problems, whereas others will require hundreds of partial waves. Coupled with this is a sum over $j = |l - \frac{1}{2}|, l + \frac{1}{2}$. There is, however, a sum over l in the ejectile wave function as well, together with a sum over j and (the source of considerable increase in computation) over m_l (the projection of l). The three-dimensional projectile and ejectile wave functions must be evaluated for every combination of quantum numbers. Additionally, the integrations over all space is nested in the integral over $\mathbf{q}$. Note also that in the distorted-wave case, the functions g_{lj} and f_{lj} are not analytical functions but must be stored in large arrays (keeping in mind the large number of quantum number combinations) further adding to the numerical burden. Together with the strong oscillatory nature of the integrand and convergence issues of the integral, it quickly becomes clear that a full partial-wave expansion is an extremely numerically intensive operation.

3. Hadronic tensor: Eikonal distorted-wave case

In contrast to the full partial-wave expansion, the Dirac eikonal distorted wave [29] offers a semianalytical form closely resembling the plane-wave expression and with the contribution of distortions effects neatly isolated in a multiplicative factor under certain conditions. Eikonal distorted-wave functions introduced by Glauber removed the computational burden of dealing with partial waves at high energies and have since been improved upon to apply to a wide range of scattering problems [30–38]. For our application, we follow the familiar procedure described by Amado [29] to derive the incoming distorted-wave function with momentum $\mathbf{k}$ to first order in the eikonal limit as

$$\psi^{(+)}(\mathbf{x}, \mathbf{k}, \hat{\mathbf{i}}, s) = \sqrt{\frac{E_{\mathbf{k}} + M}{2M}} \begin{bmatrix} \mathbf{I_2} \\ \frac{\vec{\sigma}\cdot\hat{\mathbf{p}}}{E_{\mathbf{k}} + M + V_s - V_v} \end{bmatrix} e^{i\mathbf{k}\cdot\mathbf{x}} e^{iS^{(+)}(\mathbf{x})} \phi(\hat{\mathbf{i}}, s), \tag{86}$$

where the incoming eikonal phase in cylindrical coordinates with $\mathbf{x} = (\mathbf{b}, z)$ is

$$S^{(+)}(\mathbf{b}, z) = -\frac{M}{K}\int_{-\infty}^{z} dz' \{V_c + V_{\text{so}}[\vec{\sigma}\cdot(\mathbf{b}\times\mathbf{K}) - iKz']\}, \tag{87}$$

where we have replaced the gradient operator $\hat{\mathbf{p}}$ in Eq. (87) by the average momentum defined as

$$\mathbf{K} = \tfrac{1}{2}(\mathbf{k} + \mathbf{k}'). \tag{88}$$

The central $V_c(x)$ and spin-orbit $V_{\rm so}(x)$ potentials are defined as

$$V_c(x) = V_s + \frac{E}{M}V_v + \frac{V_s^2 - V_v^2}{2M}; \tag{89}$$

$$V_{\rm so}(x) = \frac{1}{2M[E + M + V_s - V_v]}\frac{1}{x}\frac{d}{dx}[V_v - V_s], \tag{90}$$

where the Lorentz scalar $V_s(x) \equiv V_s$ and vector $V_v(x) \equiv V_v$ potentials are calculated in accordance to the prescriptions given in Ref. [39].

The outgoing eikonal distorted-wave function is derived by applying the time reversal operator $\mathcal{T}$ to the incoming wave function:

$$\psi^{(-)}(\mathbf{x}, \mathbf{k}', \hat{\mathbf{i}}', s') = \mathcal{T}[\psi^{(+)}(\mathbf{x}, \mathbf{k}', \hat{\mathbf{i}}', s')] \tag{91}$$

$$= \sqrt{\frac{E_{\mathbf{k}'} + M}{2M}}\begin{bmatrix} \mathbf{I_2} \\ \frac{\vec{\sigma}\cdot\hat{\mathbf{p}}}{E_{\mathbf{k}'} + M + V_s^* - V_v^*} \end{bmatrix} e^{i\mathbf{k}'\cdot\mathbf{x}} e^{-iS^{(-)}(\mathbf{x})} \times \sum_{s_z'} (-)^{\frac{1}{2}-s_z'} \left(\mathcal{D}^{(1/2)}_{s_z' s'}(\hat{\mathbf{i}}')\right)^* \chi_{-s_z'}, \tag{92}$$

and the outgoing eikonal phase given then by

$$S^{(-)}(\mathbf{x}) = -\frac{M}{K}\int_z^\infty dz' \{V_c^* + V_{\rm so}^*[\vec{\sigma}\cdot(\mathbf{b}\times\mathbf{K}) - iKz']\}. \tag{93}$$

In general the eikonal phases $S(\mathbf{x})$ contained in the wave functions $\psi^{(+)}$ and $\psi^{(-)}$ are 2×2 matrices acting on the Pauli spinors. However, in this work we neglect the spin-orbit potential and consequently $S(\mathbf{x})$ becomes proportional to the identity matrix. Also, before substituting Eqs. (86) and (92) into $\mathcal{H}^L(\mathbf{q})$, an additional set of approximations is made. First, for the same reasons as in Ref. [11], the gradient operators in the lower components of the Dirac spinors in Eqs. (86) and (92) are replaced by their expectation values $\mathbf{k}$ and $\mathbf{k}'$, respectively, to first order. Second, the assumption is made that $E + M$ dominates $V_s - V_v$ to such an extent that the latter can be discarded in the lower components of the incoming and outgoing Dirac eikonal distorted-wave functions. Applying these to the wave functions and substituting them into $\mathcal{H}^L(\mathbf{q})$ leads to

$$H^L(\mathbf{q}) = [\bar{U}\lambda^L U]\left\{\int b\, d^2b\, dz e^{i(\mathbf{k}-\mathbf{k}'-\mathbf{q})\cdot(\mathbf{b},z)} \times \exp\left(-i\frac{M}{K}\int_{-\infty}^{\infty} dz' V_c(\mathbf{b}, z')\right)\right\}, \tag{94}$$

where the vector $\mathbf{x} = (\mathbf{b}, z)$, and we have written the three-dimensional spatial integral d^3x in terms of cylindrical coordinates. We can recast Eq. (94) in a compact form as

$$H^L(\mathbf{q}) = [\bar{U}(\mathbf{k}', \hat{\mathbf{i}}', s')\lambda^L U(\mathbf{k}, \hat{\mathbf{i}}, s)]G(\mathbf{q}), \tag{95}$$

where

$$G(\mathbf{q}) = \int d^3x e^{i(\mathbf{k}-\mathbf{k}'-\mathbf{q})\cdot\mathbf{x}} \exp\left(-i\frac{M}{K}\int_{-\infty}^{\infty} dz' V_c(\mathbf{b}, z')\right). \tag{96}$$

Equation (95) illustrates the incredible usefulness in using eikonal distorted waves. One is able to separate all the effects related to the nuclear distortions from the effects related to the nuclear spin couplings of the particles. This form makes the eikonal approach such a powerful and insightful approximation because it allows one to systematically study these modular structures independently and assess their effects. However, Eq. (95) is again an example where the simplicity of the expression masks the complexity of the numerical implementation. The integrand contained in $G(\mathbf{q})$ is a multidimensional oscillatory integral dependent on six independent variables $b, \phi_b, z, q, \theta_q$, and ϕ_q in the case of cylindrical coordinates. Although it has a form similar to the Fourier-Bessel type eikonal scattering amplitude so regularly found in the literature, the presence of the integration variable $\mathbf{q}$ prevents further simplification of the spatial integral. In this form the integrations over z and ϕ_b now have to be explicitly performed. Even though the use of eikonal distorted-wave functions leads to greater transparency with respect to physical interpretations compared to the traditional partial-wave expansion, the point is reached where one has to resort to the numerical evaluation of specifically Eq. (96).

III. CALCULATION PROCEDURE

The integration over $\mathbf{q}$ in Eq. (58) in full reads

$$\left(\frac{d\sigma}{dE'\,d\Omega'}\right)_{\rm DW} = -\frac{1}{\pi}K\sum_{L,L'=S}^{T}|F_L(\mathbf{k}, \mathbf{K}, \mathbf{k}')|^2 \int_0^1 dq \times \int_0^1 \sin\theta_q\, d\theta_q \int_0^1 d\phi_q \times \frac{q^2}{4\pi}(q_{\rm max} - q_{\rm min})\mathcal{H}^{LL'}(q, \theta_q, \phi_q) \times {\rm Im}\{\Pi_{LL'}(q, \theta_q, \phi_q, \omega)\}, \tag{97}$$

where the appropriate transformation equation, namely,

$$\int_a^b f(x')\,dx' \to \int_0^1 f((b-a)x + a)(b-a)\,dx, \tag{98}$$

is applied to the integrals. Again, using the SS interaction only, the integral is written as

$$\left(\frac{d\sigma}{dE'\,d\Omega'}\right)_{\rm DW} = -\frac{1}{\pi}K F_S(\mathbf{k}, \mathbf{K}, \mathbf{k}')F_S^*(\mathbf{k}, \mathbf{K}, \mathbf{k}') \times \int_{q_{\rm min}}^{q_{\rm max}} dq\, F(q, \omega), \tag{99}$$

where

$$F(q, \omega) = \int_0^1 d\theta_q\, d\phi_q\ \sin\theta_q \mathcal{H}^{SS}(\mathbf{q}){\rm Im}\{\Pi_{SS}(|\mathbf{q}|, \omega)\} = {\rm Im}\{\Pi_{SS}(q, \omega)\}\int d\Omega_q \mathcal{H}^S(\mathbf{q})[\mathcal{H}^S(\mathbf{q})]^*, \tag{100}$$

and $\mathcal{H}^S(\mathbf{q})$ is given by Eq. (95) with $\lambda^L \to \lambda^S = I_4$. Equation (100) is calculated as follows:

(i) A proton with laboratory energy $T_{\rm lab} = 400$ MeV is used and is scattered off a ^{40}Ca target at a center-of-mass

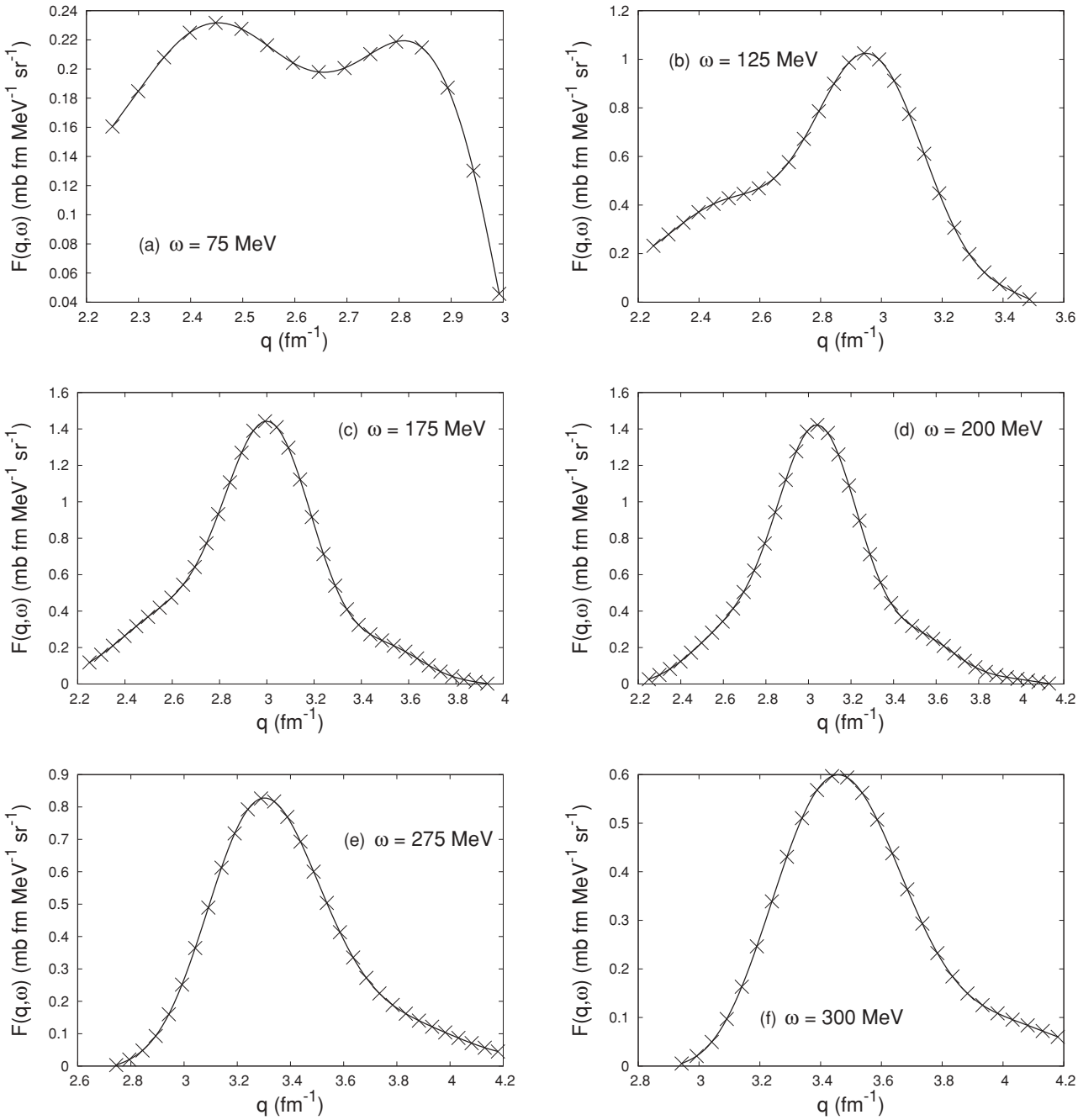

FIG. 1. Function $F(q, \omega)$ is shown with the Fourier series interpolant given in the text. The crosses indicate nonzero grid points on the q axis.

angle $\theta_{\text{c.m.}} = 40^\circ$. The incident particle has spin quantization axis and spin projection $(\hat{\mathbf{n}}, \frac{1}{2})$ and the outgoing particle $(\hat{\mathbf{n}}, \frac{1}{2})$.

(ii) An arbitrary number of "q-grid" points can be used to generate the function $F(q, \omega)$; however, for this calculation, 40 grid points typically provided sufficient nonzero values to construct an appropriately smooth $F(q, \omega)$.

(iii) Gaussian quadrature is used to compute $\mathcal{H}^S(\mathbf{q})$. To converge, this multidimensional integral requires a minimum of 50 Gaussian integration points in each dimension. Additionally, the "infinity" limits for the calculation of the eikonal phase in Eq. (96) were set to the maximum range in which the central potential $V_c \neq 0$ for a specific target. The impact parameter value $\mathbf{b}$ is set to a minimum value where the distorted wave coincides with the plane wave.

(iv) Taking the product of $\mathcal{H}^S(\mathbf{q})$ and its complex conjugate $[\mathcal{H}^S(\mathbf{q})]^*$ solves the calculation of the six-dimensional integral nested in the nine-dimensional integral of Eq. (99).

(v) Gaussian quadrature is used to compute $\int d\Omega_q \mathcal{H}^S(\mathbf{q})[\mathcal{H}^S(\mathbf{q})]^*$. To converge, this double integral (which contains the nested six-dimensional

TABLE II. Fourier coefficients for Eq. (101) used to generate the interpolant functions $F(q)$ for ten ω values.

ω	a_0		$n=1$	$n=2$	$n=3$	$n=4$	$n=5$	w
75	0.004798	a_n	0.2246	−0.07723	0.009182	0.001712	−0.0126	2.821
		b_n	0.1098	0.001151	−0.03368	0.04606	−0.009644	
100	0.1853	a_n	−0.2096	0.1054	−0.04718	0.04304	−0.003087	3.174
		b_n	0.2323	−0.005559	0.01143	−0.01069	0.0008471	
125	0.3012	a_n	−0.002143	−0.1335	0.09079	−0.007971	−0.01921	2.797
		b_n	0.4091	−0.1192	−0.0002197	0.05805	−0.01696	
150	0.3918	a_n	−0.2712	−0.01373	0.07594	−0.06597	0.01598	2.902
		b_n	0.4534	−0.2029	0.09222	−0.007007	−0.01004	
175	0.4199	a_n	−0.3609	−0.02922	0.09189	−0.06786	0.01887	2.874
		b_n	0.4586	−0.223	0.09257	−0.003499	−0.01109	
200	0.4153	a_n	−0.4845	0.07271	0.02189	−0.03825	0.01499	2.909
		b_n	0.3133	−0.226	0.1131	−0.04817	0.009294	
225	0.382	a_n	−0.5271	0.2177	−0.0857	0.04091	−0.009284	3.006
		b_n	0.005177	−0.06416	0.03843	−0.01847	0.004432	
250	0.3157	a_n	−0.4063	0.1814	−0.06474	0.0199	−0.004281	3.036
		b_n	−0.1786	0.08986	−0.04264	0.02192	−0.004418	
275	0.9568	a_n	−0.2865	−0.934	0.3436	0.05794	−0.06808	2.189
		b_n	−1.088	0.7291	0.4096	−0.245	−0.04082	
300	6.977	a_n	−12.24	9.047	−4.893	1.886	−0.446	1.693
		b_n	−0.3726	0.2234	−0.1646	−0.08791	−0.01425	

integral of above) requires a minimum of 60 Gaussian integration points in each dimension. This numerical integration step effectively computes the eight-dimensional integral $F(q,\omega)$.

(vi) We employ the powerful MATLAB **cftool** package to fit $F(q,\omega)$.

(vii) For each value of ω we find that for this calculation, $F(q,\omega)$ is well reproduced by the following Fourier series

$$F(q,\omega) = \frac{a_0}{2} + \sum_{n=1}^{5}[a_n \cos(nwq) + b_n \sin(nwq)], \tag{101}$$

where the ω-dependent coefficients for this calculation are given in Table II. As an example, the interpolation procedure is shown in Fig. 1.

By substituting Eq. (101) into Eq. (99) the analytical expression for the polarized double differential cross section is then

$$\begin{aligned}\frac{d\sigma}{dE'\,d\Omega'} &= \sum_{n=1}^{5}\int_{q_{\min}}^{q_{\max}} dq\left(\frac{a_0}{2} + [a_n\cos(nwq) + b_n\sin(nwq)]\right)\\ &= \frac{a_0(\omega)}{2}(q_{\max}-q_{\min}) + \sum_{n=1}^{5}\left\{\frac{b_n(\omega)}{nw}[\cos(nwq_{\min})\right.\\ &\quad \left. - \cos(nwq_{\max})] + \frac{a_n(\omega)}{nw}[\sin(nwq_{\max}) - \sin(nwq_{\min})]\right\},\end{aligned} \tag{102}$$

and we can use Eq. (102) to calculate the double differential cross section for each value of ω. Figure 4 shows the unpolarized double differential cross section for the plane-wave calculation for the rank-0 polarizations compared to the unpolarized double differential cross section for the distorted-wave calculation for the rank-0 polarization. This result our attempt to calculate the distorted-wave double differential cross section for quasielastic scattering.

IV. RESULTS

The results using the derived expression for the polarized double differential cross section for quasielastic scattering in the plane-wave case for the *SS* interaction given in Eq. (75) are shown in Figs. 2(a) and 2(b) shows that for the *PP* interaction.

Our calculations of the polarized double differential cross sections presented in Figs. 2(a) and 2(b) are for an incident proton with $T_{\rm lab} = 400$ MeV scattering off a ^{40}Ca target at $\theta_{\rm c.m.} = 40^\circ$ with incoming quantization axis s and outgoing axis s'. For the polarization orientations using the short-hand notation to indicate the spin projections, one finds that the magnitudes of the uu and dd differential cross sections are equal and lie on top of each other in Fig. 2, hence only one curve is visible for the two cross sections in the plot. This trend is the same for the du and ud directions; however, the magnitude for these projections is smaller than for the uu and dd projections. In the calculation the quasielastic peak is located at an energy transfer $\omega = 175$ MeV for all the polarized differential cross section cases. We summarize this result as follows: For the case with incoming quantization axis $\hat{\mathbf{s}}$ and outgoing axis $\hat{\mathbf{s}}'$ denoted as $(\hat{\mathbf{s}},\hat{\mathbf{s}}')$, the respective magnitudes are denoted

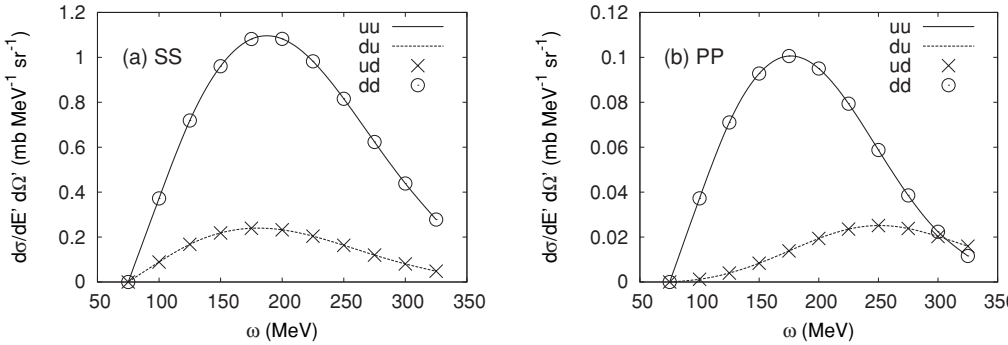

FIG. 2. Polarized double differential cross sections for the plane-wave case for the $\hat{\mathbf{s}}$ and $\hat{\mathbf{s}}'$ quantization directions at $T_{\rm lab} = 400$ MeV on ^{40}Ca, $\theta_{\rm c.m.} = 40^\circ$. In the $(\hat{s}, \hat{s}')$ polarized differential cross sections, the uu and dd states are equal and $du = ud$, hence only two sets of curves are visible in the plots.

as $uu = dd > du = ud$, as explained above, and the location of the respective quasielastic peaks as $uu = dd = du = ud$. Table III summarizes the results for the other quantization directions for the *SS* and *PP* interactions.

In Table III the polarization directions $(\hat{\mathbf{n}}, \hat{\mathbf{n}})$ have only one set of polarized nonzero differential cross sections, namely, uu and dd for the *SS* interaction and du and ud for the PP interaction; hence the comparison of the relative positions of the quasielastic peak for these polarizations become redundant. From the table one finds that $(\hat{\mathbf{l}}, \hat{\mathbf{l}}')$ and $(\hat{\mathbf{s}}, \hat{\mathbf{s}}')$ have equal profiles for the *SS* interaction; however, "flipped" profiles for the PP interaction. These two polarizations represent a $\pi/2$ rotation difference and for a spherical symmetric potential, as in these calculations, the result is consistent and expected. Similarly, for the *SS* interaction, the $(\hat{\mathbf{l}}, \hat{\mathbf{s}}')$ and $(\hat{\mathbf{s}}, \hat{\mathbf{l}}')$ profiles are flipped for the magnitudes. For the PP interaction and both polarization directions $(\hat{\mathbf{l}}, \hat{\mathbf{s}}')$ and $(\hat{\mathbf{s}}, \hat{\mathbf{l}}')$, the magnitudes and positions of the quasielastic peaks are identical and is a consistent result for the spherically symmetric target nucleus used in the calculations.

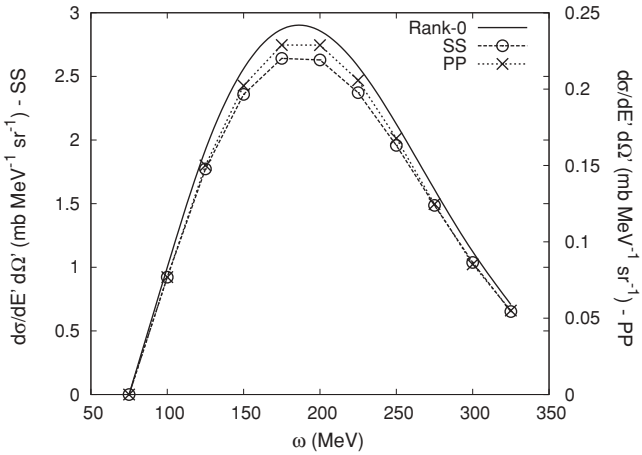

FIG. 3. Unpolarized double differential cross sections for the *SS* interaction, the *PP* interaction, and the rank-0 polarization for the plane-wave calculation with $T_{\rm lab} = 400$ MeV proton on ^{40}Ca at $\theta_{\rm c.m.} = 40^\circ$. The scale on the left of the plot refers to the *SS* calculation and that for the *PP* calculation is shown on the right. Note that the *PP* differential cross section is an order of magnitude smaller than that for the *SS* calculation.

As stated previously, the unpolarized double differential cross section is given by the denominator in Eq. (82) and is shown for the *SS* (circle-dashed) and *PP* (cross-dotted) interactions in Fig. 3. The sum of the four unpolarized differential cross sections,

$$\left(\frac{d\sigma}{dE'\,d\Omega'}\right)_{\text{rank-0}} = \left(\frac{d\sigma}{dE'\,d\Omega'}\right)_{SS} + \left(\frac{d\sigma}{dE'\,d\Omega'}\right)_{SP} + \left(\frac{d\sigma}{dE'\,d\Omega'}\right)_{PS} + \left(\frac{d\sigma}{dE'\,d\Omega'}\right)_{PP}, \tag{103}$$

where each double differential cross section in Eq. (103) on the right-hand side is the *unpolarized* double differential cross

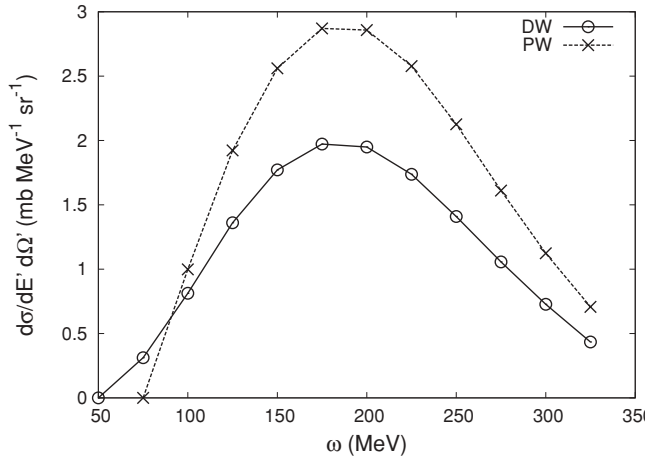

FIG. 4. Unpolarized rank-0 double differential cross sections for the plane-wave (PW) and distorted-wave (DW) calculations. The differential cross sections are for the incoming $\hat{\mathbf{n}}$ and outgoing $\hat{\mathbf{n}}$ quantization directions at $T_{\rm lab} = 400$ MeV on ^{40}Ca, $\theta_{\rm c.m.} = 40^\circ$. Each circle in the distorted-wave double differential cross section is the integral value of each interpolation function shown in Fig. 1. Note that the distorted-wave calculation is above the plane-wave calculation at lower momentum transfer values, as this is a consequence of using Eq. (74) as opposed to a numerical evaluation of $\delta(0)$. This factor for $\delta(0)$ leads to the sharp cutoff of the plane-wave calculation at lower momentum transfer values and is not a result of nuclear distortions seemingly having an opposite effect at lower momentum transfer values.

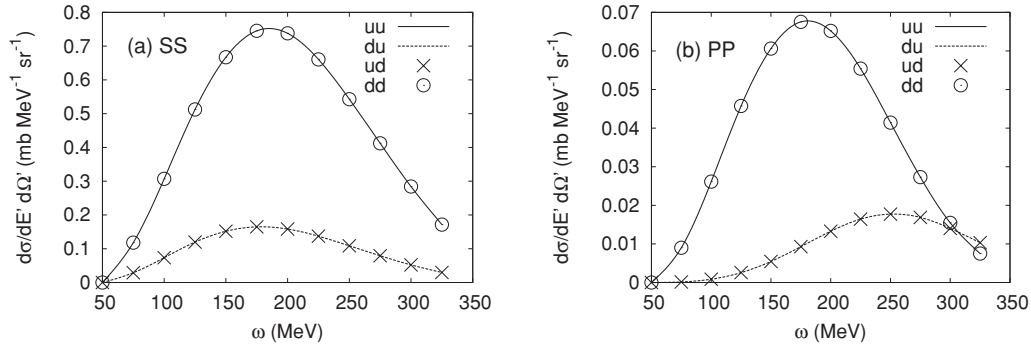

FIG. 5. Polarized double differential cross sections for the distorted-wave case for the s and s' quantization directions at $T_{\rm lab} = 400$ MeV on ^{40}Ca, $\theta_{\rm c.m.} = 40^\circ$. In the $(\hat{s}, \hat{s}')$ polarized differential cross sections, the uu and dd states are equal and $du = ud$, hence only two sets of curves are visible in the plots.

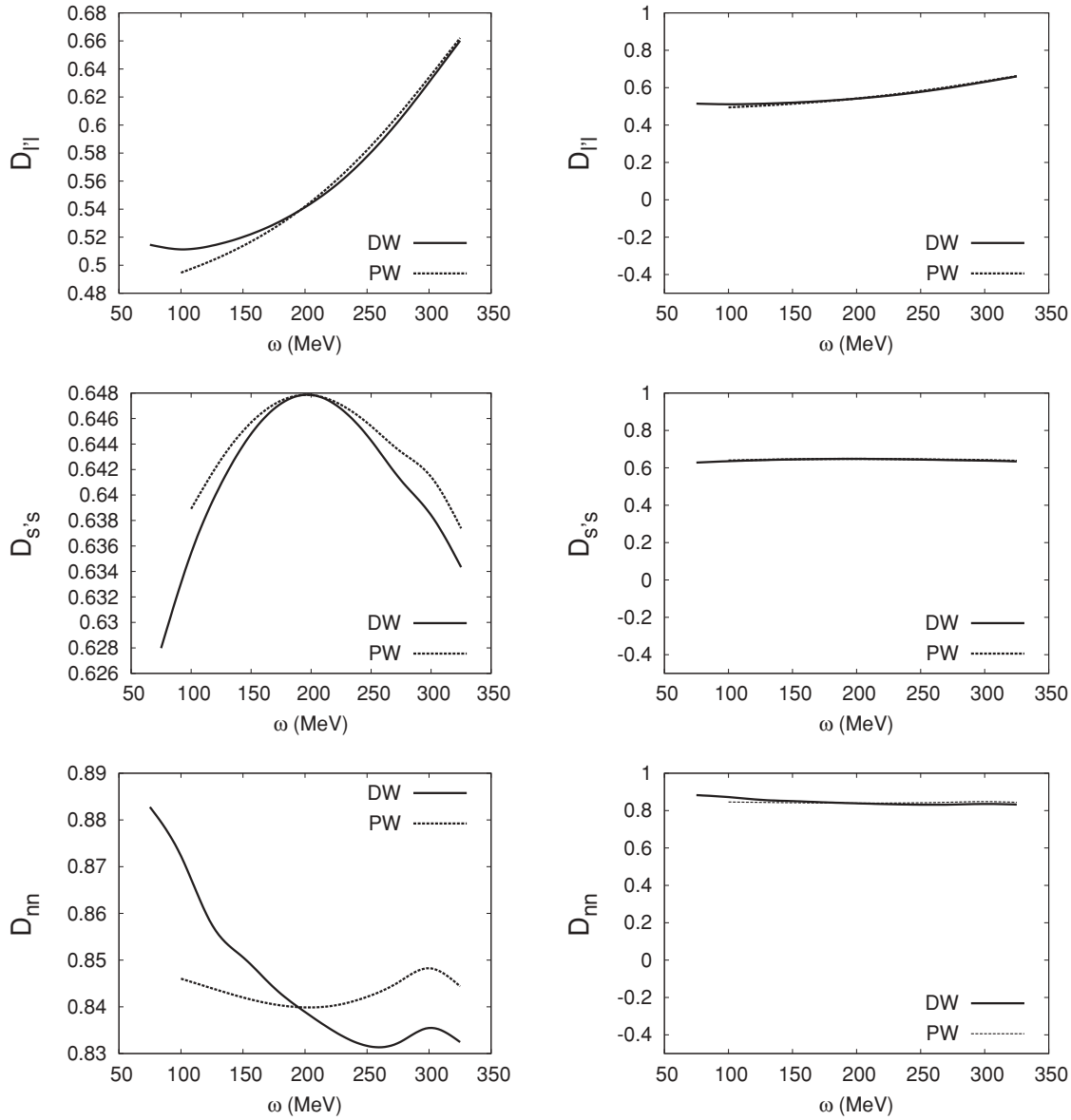

FIG. 6. Plane-wave and distorted-wave spin observable values for $D_{l'l}$, $D_{s's}$, and D_{nn} for protons with laboratory incident energy of $T_{\rm lab} = 400$ MeV on ^{40}Ca for quasielastic scattering at $\theta_{\rm c.m.} = 40^\circ$. The figures on the right are presentations in which the vertical axes have been expanded in relation to the plots to their immediate left.

TABLE III. Magnitude and position comparison for the polarized differential cross sections for the plane-wave calculations for the different polarization directions. These polarized double differential cross sections are used to compute the unpolarized double differential cross sections and spin observables.

Polarization		*SS*	*PP*
$(\hat{\mathbf{l}}, \hat{\mathbf{l}}')$	Magnitude	$uu = dd > du = ud$	$uu = dd < du = ud$
	Position	$uu = dd = du = ud$	$uu = dd > du = ud$
$(\hat{\mathbf{s}}, \hat{\mathbf{s}}')$	Magnitude	$uu = dd > du = ud$	$uu = dd > du = ud$
	Position	$uu = dd = du = ud$	$uu = dd < du = ud$
$(\hat{\mathbf{n}}, \hat{\mathbf{n}})$	Magnitude	$uu = dd > du = ud = 0$	$uu = dd = 0 < du = ud$
	Position	–	–
$(\hat{\mathbf{l}}, \hat{\mathbf{s}}')$	Magnitude	$uu = dd < du = ud$	$uu = dd < du = ud$
	Position	$uu = dd = du = ud$	$uu = dd < du = ud$
$(\hat{\mathbf{s}}, \hat{\mathbf{l}}')$	Magnitude	$uu = dd > du = ud$	$uu = dd < du = ud$
	Position	$uu = dd = du = ud$	$uu = dd < du = ud$

section, generates the unpolarized rank-0 double differential cross section. One therefore needs a total of 16 polarized double differential cross sections to compute the rank-0 differential cross section. The solid line in Fig. 3 indicates the unpolarized rank-0 differential cross section. Clearly, the *SS* cross section dominates and contributes more the 90% of the unpolarized rank-0 differential cross section.

The relationship between the plane-wave calculation and the distorted-wave calculation is essentially contained in the hadronic tensor and is given by Eq. (95). The effect the multiplicative factor $G(\mathbf{q})$ has on the differential cross section is to reduce its magnitude in the distorted-wave case and is shown in Fig. 4.

In using the expression for $\delta(0)$ given in Eq. (74), the plane-wave calculation has a sharp cutoff at lower momentum transfer values. The result of this is that the plane-wave calculation is now below the distorted-wave calculation and is therefore not an opposite effect of distortions at lower momentum transfer values. This result represents a successful calculation of the distorted-wave quasielastic differential cross section for proton-nucleus scattering within a full relativistic framework. The mixing of polarization states is controlled by the proportionality factor $[\bar{U}\lambda^L U]$ and yields the same relationships given in Table III for the distorted-wave case. To illustrate this result, Fig. 5 shows the *distorted*-wave polarized double differential cross sections for the polarization directions $(\hat{\mathbf{s}}, \hat{\mathbf{s}}')$.

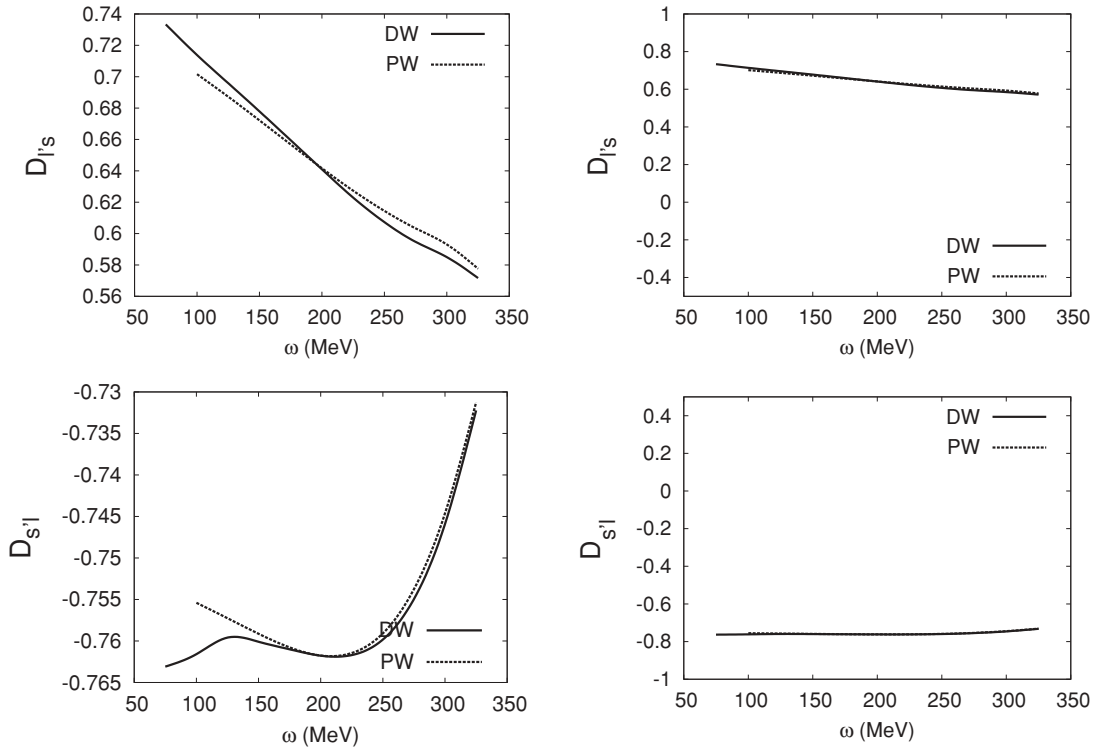

FIG. 7. Same as Fig. 6, but for spin observables $D_{l's}$ and $D_{s'l}$.

Comparing the distorted-wave calculation with those for the plane-wave calculation (Fig. 5 vs Fig. 3), the magnitude differences between different polarization directions are equal, as are the locations of the quasielastic peaks.

In contrast to the differential cross sections of the distorted-wave calculation which are similar to that for the plane-wave calculation, the spin observables are very interesting.

In Figs. 6 and 7 the figures on the right show spin observables as they are normally presented in the literature. One notices that these observables are flat; however, when one changes the scale on the vertical axis, there is substantial structure in the curves. None of the spin observables show similar structure, and therefore their interpretation becomes difficult. What is clear, however, is that there is very little influence of distortion on spin observables.

V. CONCLUSION

In this paper we have developed a relativistic formalism that calculates the quasielastic polarized double differential cross section using plane waves and an attempt is made using distorted waves. We find that the simple mathematical structure of the contraction of two tensors to calculate the differential cross section also holds when distortions are included in the formulism. The effect distortions have on the differential cross section is to reduce the magnitude of the differential cross section. The general structure and features of the polarized differential cross sections are preserved and are identical for the plane-wave and distorted-wave calculations. This is because the distortions enter as a multiplicative factor in the differential cross section. The proportionality factor in the differential cross section contains the polarized incoming and outgoing Dirac spinors and in contrast controls the polarization state mixing in the case of the rank-0 calculations. Furthermore, using the rank-0 unpolarized differential cross sections, the plane-wave and distorted-wave spin observables were calculated and compared, and one can conclude that distortions have a negligible effect on spin observables for the rank-0 case.

ACKNOWLEDGMENTS

N.P.T acknowledges the Namibia Government Scholarship & Training Program (NGSTP) for their generous financial support. B.I.S. v.d.V acknowledges the financial support of the National Research Foundation of South Africa under Grant No. GUN 2048567.

[1] C. J. Horowitz and D. P. Murdock, Phys. Rev. C **37**, 2032 (1988).
[2] G. C. Hillhouse and P. R. De Kock, Phys. Rev. C **49**, 391 (1994).
[3] G. C. Hillhouse and P. R. De Kock, Phys. Rev. C **52**, 2796 (1995).
[4] B. I. S. van der Ventel, G. C. Hillhouse, and P. R. De Kock, in *Proceedings of RCNP International Symposium on Nuclear Responses and Medium Effects, Osaka, Japan, November 1998*, edited by T. Noro, H. Sakaguchi, H. Sakai, and T. Wakasa (Universal Academy, Tokyo, 1999), p. 183.
[5] G. C. Hillhouse, B. I. S. van der Ventel, S. M. Wyngaardt, and P. R. De Kock, Phys. Rev. C **57**, 448 (1998).
[6] B. I. S. van der Ventel, G. C. Hillhouse, P. R. De Kock, and S. J. Wallace, Phys. Rev. C **60**, 064618 (1999).
[7] B. I. S. van der Ventel, G. C. Hillhouse, and P. R. De Kock, Phys. Rev. C **62**, 024609 (2000).
[8] C. J. Horowitz and J. Piekarewicz, Phys. Rev. C **50**, 2540 (1994).
[9] C. J. Horowitz and M. J. Iqbal, Phys. Rev. C **33**, 2059 (1986).
[10] J. R. Shepard, E. Rost, and J. Piekarewicz, Phys. Rev. C **30**, 1604 (1984).
[11] J. Piekarewicz, Phys. Rev. C **32**, 1693 (1985).
[12] B. Van Overmeire, W. Cosyn, P. Lava, and J. Ryckebusch, Phys. Rev. C **73**, 064603 (2006).
[13] D. Debruyne, J. Ryckebusch, W. Van Nespen, and S. Janssen, Phys. Rev. C **62**, 024611 (2000).
[14] J. D. Bjorken and S. D. Drell, *Relativistic Quantum Mechanics* (McGraw-Hill, New York, 1965).
[15] W. Greiner, *Quantum Chromodynamics* (Springer-Verlag, Berlin, 1994).
[16] D. L. Adams and M. Bleszynski, Phys. Lett. B **136**, 10 (1984).
[17] T. Matsui and B. D. Serot, Ann. Phys. (NY) **144**, 107 (1982).
[18] J. R. Shepard, J. A. McNeil, and S. J. Wallace, Phys. Rev. Lett. **50**, 1443 (1983).
[19] J. A. McNeil, J. R. Shepard, and S. J. Wallace, Phys. Rev. Lett. **50**, 1439 (1983).
[20] J. Piekarewicz, R. D. Amado, and D. A. Sparrow, Phys. Rev. C **32**, 949 (1985).
[21] R. A. Arndt and D. Roper, VPI and SU Scattering Analysis Interactive Dial In Program and Data Base (unpublished).
[22] J. J. Sakurai, *Modern Quantum Mechanics*, 2nd ed. (Addison-Wesley, New York, 1993).
[23] K. Wehrberger, Phys. Rep. **225**, 273 (1993).
[24] D. D. van Niekerk, Ph.D. thesis, University of Stellenbosch, 2010.
[25] B. I. S. van der Ventel, Ph.D. thesis, University of Stellenbosch, 1999.
[26] G. C. Hillhouse, Ph.D. thesis, University of Stellenbosch, 1999.
[27] E. Rost, J. R. Shepard, E. R. Siciliano, and J. A. McNeil, Phys. Rev. C **29**, 209 (1984).
[28] E. Rost and J. R. Shepard, Phys. Rev. C **35**, 681 (1987).
[29] R. D. Amado, J. Piekarewicz, D. A. Sparrow, and J. A. McNeil, Phys. Rev. C **28**, 1663 (1983).
[30] R. J. Glauber, in *Lectures in Theoretical Physics*, edited by W. E. Brittin and L .G. Dunham, Vol. 1 (Interscience, New York, 1959), p. 315.
[31] S. J. Wallace, Ann. Phys. (NY) **78**, 190 (1973).
[32] S. J. Wallace, Phys. Rev. D **8**, 1934 (1973).
[33] A. Baker, Phys. Rev. D **8**, 1937 (1973).
[34] R. D. Amado, J. P. Dedonder, and F. Lenz, Phys. Rev. C **21**, 647 (1980).
[35] R. D. Amado, J. Piekarewicz, D. A. Sparrow, and J. A. McNeil, Phys. Rev. C **29**, 936 (1984).
[36] D. Waxman, C. Wilkin, J.-F. Germond, and R. J. Lombard, Phys. Rev. C **24**, 578 (1981).
[37] T. W. Chen, Phys. Rev. C **30**, 585 (1984).
[38] S. J. Wallace and J. L. Friar, Phys. Rev. C **29**, 956 (1984).
[39] S. Hama, B. C. Clark, E. D. Cooper, H. S. Sherif, and R. L. Mercer, Phys. Rev. C **41**, 2737 (1990).